Synthesis by Microwaves of Bimetallic Nano-Rhodium-Palladium

u. Ugalde, E. Chavira, M.T. Ochoa-Lara, I.a. Figueroa, C. Quintanar, and A. Tejeda

Abstract

An improved acrylamide sol-gel technique using a microwave oven in order to synthesize bimetallic Rh-Pd particles is reported and discussed. The synthesis of Pd and Rh nanoparticles was carried out separately. The polymerization to form the gel of both Rh and Pd was carried out at 80°C under constant agitations. The method chosen to prepare the Rh and Pd xerogels involved the decomposition of both gels. The process begins by steadily increasing the temperature of the gel inside a microwave oven (from 80°C to 170°C). In order to eliminate the by-products generated during the sol-gel reaction, a heat treatment at a temperature of 1000°C for 2 h in inert atmosphere was carried out. After the heat treatment, the particle size increased from 50 nm to 200 nm, producing the bimetallic Rh-Pd clusters. It can be concluded that the reported microwave-assisted, sol-gel method was able to obtain nano-bimetallic Rh-Pd particles with an average size of 75 nm.

Introduction

Bimetallic alloy (solid solutions or intermetallics compounds) nanostructures, synthesized from two single components, have been of interest because of their superior properties, in comparison with their respective single-component species, that is, Ag, Pd, Rh, and so forth [1]. The synthesis of noble metals and alloys, in nanometric scale, has been extensively investigated in nanotechnology because of their optical and electronic properties, as well as for their useful applications in many fields such as medicine [2], catalysis, and sensors [3–6].Hardness, highmelting and boiling points, and

high thermal and electrical conductivity are some of the existing properties of these noble metals.

Rhodium and palladium (Rh and Pd) crystallize in a face centered cubic (fcc) unit cell. Both metals add s electrons to the collective d band of palladium [7] and increase the lattice parameter of the palladium host lattice [8, 9]. It was found that rhodium behaves as an absorber of hydrogen at high pressure of gaseous hydrogen when situated within the palladium lattice [10, 11].

Recently, Pd nanocrystals have been prepared in aqueous solutions giving rise to a great variety of shapes, including truncated octahedron, cube, octahedron, and thin plate [12–14], making them ideal candidates as seeds for growing bimetallic nanostructures. The control of crystal size and its dispersion are among the main goals of nanocrystal preparation. This is due to the physicochemical properties of a bimetallic nanocrystal that can be tailored by controlling their particle size, shape, and elemental composition, as well as their internal and surface structures. Recently, the complexity of nanomaterials can be further enhanced by the formation of multimetallic nanostructures (e.g., coreshell and dumbbell). Synthesis parameters such as capping agent, metal ion, and reaction temperature also play an important role in the overgrowth process [15]. Among the available methods to obtain nanosized bimetallic particles of rhodium-palladium are the coimpregnation method [16, 17], nanocrystals stabilized in micelles, [18, 19] gas evaporation [20, 21] polyol process [22], and the sol-gel method [23].

Differentmethods have been developed to producemetal nanoparticles, but these differ significantly, depending on the application required. Osseo-Asare and Arriagada [18] stabilized Rh particles using the ionic (poly (N-vinyl-2- pyrrolidone)-co-(1-vinyl-3-

alkylimidazolium halide)) copolymer in ionic solvents. They found a distribution of particles of ~3 ± 0.6 nm. These nanoparticles were used as catalysts for arene hydrogenation. Similarly, Pileni [19] produced Rh nanoparticles through chemical reduction. This synthesis method is widely used to produce nanoparticles, which will be used as catalysts, on an industrial scale. They reported that the Rh nanoparticles are formed by reducing Rh ions in ethanol-water solvent with the polymers of polyvinylpyrrolidone (PVP) [20, 21]. The PVP encapsulates the nanoparticles in the solution and prevents their accumulation. The growth of the nanoparticles may be limited during the reduction by the space restrictions imposed by the three-dimensional PVP network. The particles generated from this method showed an average size of 3.2 ± 0.7 nm. However, it was noted that within the network of the Rh-PVP, therewere Cl atoms.These species came from the reagent used ($RhCl_3$ ($_3H_2O$)). During the synthesis, the Cl atoms were entrapped as an impurity in the interlattice planes of the material.The particles produced can only be used for catalysis, since the aforementioned reagent stabilizes them.Thus, the impurities anchored in the structure may detrimentally affect their catalytic properties. Therefore, it is imperative to produce impurity-free Rh, Pd, or Rh-Pd nanoparticles, in order to widen their possible applications [24–42].

Based on the above, the objective of this work is to synthesize an impurities-free bimetallic alloy of palladiumrhodiumthrough amodified polyacrylamide sol-gelmethod, using microwave radiation. The motivation of this study is based on the observation that a possible synergismmay exist between both metallic atoms, as they are located in close proximity. The possible union effect can be reflected in the chemical performances of both metals, which differ from the chemical behavior of each of the

metallic components alone. Finally, it is worthmentioning that sol-gelmethod was chosen because nanoparticle size control can be achieved by means of heat treatments or pH variations.

Experimental Procedure

Materials and Synthesis Procedure: The reagents used in this work were Rhodium metal (99.9%, Sigma-Aldrich), Palladium acetate ($Pd(OAc)_2$ 99%, Aldrich), sulfuric acid (H_2SO_4, J. T. Baker), nitric acid (HNO3; 70%, J. T. Baker), ammonium hydroxide (NH_4OH; 28–30%, J. T. Baker), ethylenediaminetetraacetic acid (EDTA; 99%, Fluka), N,N'-methylenebisacrylamide (99.5%, Fluka), 2,2'-azobis(2-methylpropionamidine) dihydrochloride (98%, Fluka), acrylamide monomer (99%, Sigma-Aldrich), and distilled water.

The synthesis of Pd and Rh nanoparticles was carried out separately, using an acrylamide sol-gel technique [43]. The synthesis of Rh nanoparticles started dissolving 439mmoL of Rh metal in H_2SO_4 and distilled water (80 mL) at 70∘C, forming a yellowish solution. Later, the solution was cooled down to ambient temperature prior to adjusting the pH ca. to 7 by adding NH_4OH, following the method outlined in [44]. As soon as a pH ca. 7 was reached, the solution was heated up to 80∘C, and 51.6mmoL of EDTA was added to complex the rhodium ions, avoiding the formation of agglomerates. After this, 211mmoL of acrylamide monomer and 9.72mmoL of cross-linking agent, N,N' methylenebisacrylamide, were added to the initial solution. Finally, to produce the gel, 5.5mmoL of initiator, 2,2'-azobis(2-methylpropionamidine)dihydrochloride, was added to reach the polymerization [43]. The pH of the solution was constantly monitored by means of a pH meter (Thermo Scientific Orion star A221). The polymerization of Rh

was carried out at 80°C under constant agitation. It is worth noting that all the processes were done under air atmosphere. In neutral or basic conditions, the time required to form the gel decreases considerably [26].

The synthesis of Pd nanoparticles was carried out by dissolving Pd acetate in 300mL of distilled water, at 80°C. After this, 12mL of HNO_3 and H_2O_2 were added. Later, the solution was cooled down to ambient temperature prior to adjusting the pH ca. to 7 by adding NH_4OH, similar to the method used for Rh. As soon as a pH ca. 7 was reached, the solutionwas heated up to 80°C, and 10.2mmoL of EDTAwas added. This EDTA reagent is used in this process with the aim of trapping the Pdmetal ions and preventing the formation of agglomerates, until the reaction starts. By doing this, the Pd ions remain stable during the decomposition of EDTA [43].

In order to start the polymerization, 562.7mmoL of acrylamide monomer and 129.7mmoL of the cross-linker N–N' methylenebisacrylamide were added. Immediately, 3.68mmoL of a chemical initiator α–α' azodiisobutyramidine dihydrochloride was incorporated to the solution in order to increase interconnection velocity [43, 44]. The polymerization occurred at 80°C in air, under continuous magnetic stirring.

The method chosen to prepare the Rh and Pd xerogels involves the decomposition of both gels. The process begins by heating up both gels inside a microwave oven, that is, from 80°C to 170°C. The microwave is equipped with an infrared temperature sensor, installed in such fashion that it can measure the temperature of the material, in analysis, within the reaction area. In this process, the oven increases the temperature steadily. Once a temperature of 170°C has been

reached (under an argon flux), the process to generate the xerogel of Rh and Pd lasts 30min and 3min, respectively. The produced Rh and Pd xerogels were pulverized, using an agate electric mortar (Retsch GmbH-Mortar Grinder RM 100), and heated at 1000 ± 4°C for 2 h, under an argon flux.

Characterization: The crystalline structure of the materials produced was determined by XRD, using a Bruker AXS D8-advance diffractometer, with Cu Kα radiation (λ = 1.5406 Å), 40 KV and 30mA, equipped with a graphite diffracted beam monochromator. The diffractogram patterns were collected at room temperature over the 2θ range to 70°, with a step size of 0.02°, and time per step of 0.6 s. A thermal analyzer (STD Q600, TA-Instruments) using a standard alumina pan, with a heating rate of 10°Cmin^{-1} in air atmosphere, over a range of temperatures of 30°C to 1000°C was used to study decomposition temperatures.

The microstructure and morphology were observed using a scanning electron microscope (SEM JSM5800L, JEOL) and a high-resolution transmission electron microscope (HRTEM JEM-2200FS, JEOL). The samples were prepared by dispersing ca. 2mg of Rh-Pd nanocrystals in 4mL of 1- propanol and were then sonicated for 15min. Finally, a drop of dispersion was deposited on a lacey carbon supported copper grid (200 mesh). A series of SEM micrographs, at 10kV, and HR-TEM, at 200kV, were taken. The composition of the material was determined with an Energy Dispersive X-Ray (EDX) spectroscope, with an Oxford Incax-sight 7688 detector. The size distribution was determined from the micrographs taken with the HRTEM. The size distribution histograms were calculated using “Image J” software (Image Processing and Analysis in

Java). In this work, the diameters of at least 100 particles were measured and mean values were determined. The statistical error was also included.

Results and Discussion

X-Ray Diffraction Patterns: The combination of the XRD and TGA analysis proved to be useful when observing the number of phases that changed during the applied heat treatments to the gel and xerogel. Figure 1(a) shows the gel and xerogel diffractograms of Rh. Both diffractograms showed the presence of two distinctive crystalline phases, that is, ammoniumsulfate $(NH_4)_2SO_4$ (PDF 01-78-0579) and edetic acid$C_{10}H_{16}N_20_8$ (PDF 00-033-1672).The former could be attributed to the addition of NH_4OH, which was used to neutralize pH of the solution in the reaction. The latter could be associated with the reaction between the polymer and the EDTA. The xerogel diffractogram clearly shows six low intensity peaks that correspond to edetic acid; this evidences that the edetic acid is being removed during this process.

The Pd diffraction patterns of the xerogel and gel products are displayed in Figure 1(b). The Pd gel showed a typical halo for amorphous materials. It is thought that this material has been produced by the remained amount of acrylamide polymer, although a small Bragg peak was observed at ~2θ = 40°. This low intensity peak could be attributed to Pd (PDF 03-065-6174). On the other hand, the Pd xerogel diffractogram not only showed the amorphous contribution and the peak that corresponds to Pd but also displayed a number of peaks that were identified as palladium oxide (PdO) (PDF 01-075-0584), Pd $(NO_3)_2(H_2O)_2$(PDF 01-085-2483), and NH_4NO_3 (PDF 00-08-0452). It is thought that these compounds are the product of the transformation of the gel to xerogel.

After the heat treatment at 1000°C for 2 h, all by-products shown inFigures 1(a) and 1(b) disappeared.This can be clearly observed in Figure 1(c), where only the peaks of Pd (PDF 03-065-6174) and Rh (PDF 01-087-0714) metallic elements are displayed. Therefore, the formation of the bimetallic compound Rh-Pd is supported by these results.

Thermogravimetric Analysis (TGA): The TGA curves are important to determine the temperatures to which the formation of organic matter and subproducts take place during the sol-gel synthesis. The results obtained from this technique did help to control the process parameters to produce the Rh-Pd bimetallic material.

The TGA results obtained from the rhodium and palladium gel and xerogel were analyzed separately and are shown in Figure 2. The TGA gel and xerogel traces for rhodium (Figure 2(a)) showed a weight loss at ~230°C and 241°C, respectively, indicating that there was a process of polymer degradation.The removal of $(NH_4)_2SO_4$ occurred at 328°C in the gel and at 378°C in xerogel. It was also observed that the formation of Rh_2O_3 occurred at 597°C and 620°C for the gel and xerogel, respectively. When increasing the temperature up to 1000°C, particles of Rh were obtained, confirming the elimination of all by-products generated before and during heat treatment.

Figure 2(b) exhibits the thermograms for the Pd gel and xerogel. For the Pd gel, an initial weight loss at 148°C was evident. This was attributed to the evaporation of H_2O, while at 260°C the weight loss corresponded to the removal of NH_4NO_3. Similarly, at 400°C, the elimination of Pd $(NO_3)_2(H_2O)_2$ compound is detected, and finally at 505°C

the decomposition of PdO was observed.The TGA for the Pd. xerogel curve displays aweight loss at 293°C, as a consequence of the degradation of both the acrylamide and NH_4NO_3 Compounds. Some ($Pd(NO_3)_2(H_2O)_2$) traces were detected around 400°C, and then, the observed drop of theTGAcurve at 557°C indicates that after this temperature, the formation of Pd particles can be favored.

From these results and considering the decomposition points of Rh_2O_3 and PdO, both compounds were heat treated at 1000°C for 2 h under an Ar flux. After this, it was expected that the growth of those Pd-Rh particles might occur. Table 1 shows the average of weight loss obtained by means of thermal analysis.

Scanning Electron Microscopy (SEM): Figure 3(a) shows the bimetallic material before being subjected to the heat treatment at 1000°C. This image clearly shows a morphology mainly composed by elongated granules ranging from 500 nm to 1 μm. Figure 3(b) shows the morphology of the bimetallic Rh-Pd grains produced after applying the heat treatment; it was observed that the material started to grow, forming sphero-hexagonal shapes between 1 and 7 μm. The EDS elemental analysis of the Rh-Pd particles is shown in Figure 4. The average composition percentage for the Rh and Pd was 34.53% and 65.47%, respectively. Figure 5 shows the elemental SEM mapping performed to the produced Rh-Pd particles. This analysis confirmed the homogeneous distributions of the Rh and Pd elements in thematerial.

High Resolution Transmission Electron Microscopy (HRTEM): In order to observe the Rh-Pd particles by HRTEM, these were dispersed by ultrasonication. The HRTEM micrographs showed the formation of clusters with a polyhedron shape and distribution

of the grains' size ranging from 50 to 200nm (Figure 6(a)). Figure 6(c) shows the micrograph of one Rh-Pd particle with a size of ~100 nm. It is thought that the change in size and geometry of those particles could be attributed to the sonication process, which fractured and broke the sphero-hexagonal shape particles, producing nano-hexagonal shapes particles, with an average size of 75 nm, as shown in Figure 6(b).

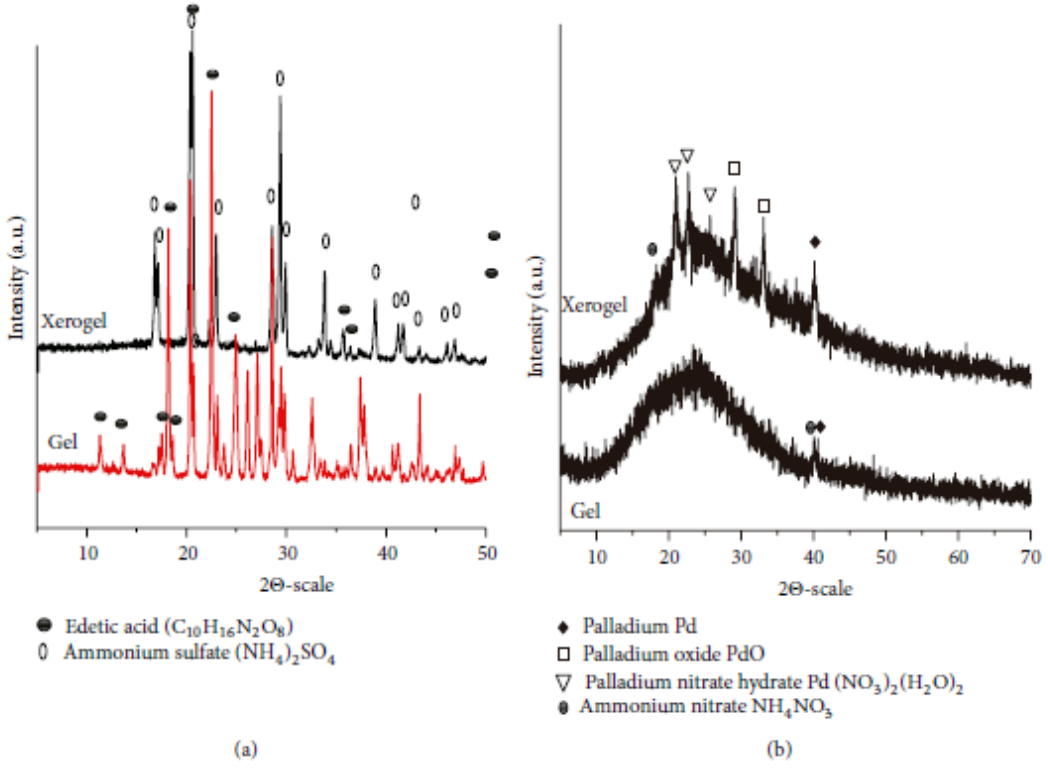

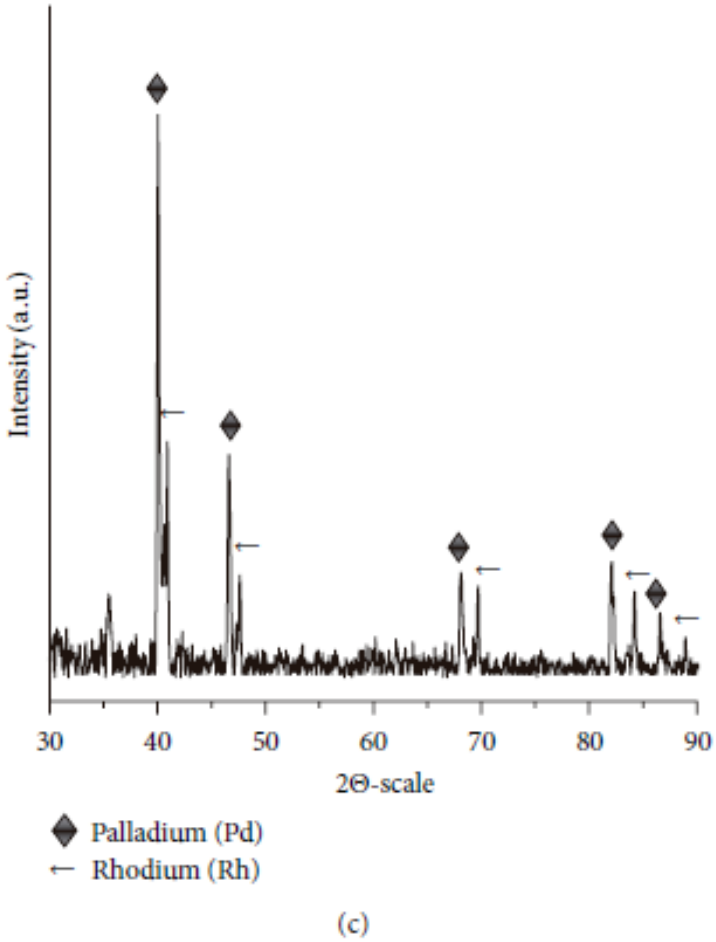

FIGURE 1: XRD patterns of (a) Rh, (b) Pd, and (c) bimetallic Rh-Pd.

The results presented in this work for the synthesis of bimetallic Rh-Pd by sol-gel with acrylamide using microwaves were in good agreement with those reported in [45, 46]. They reported the synthesis of Pd-Rh bimetallic nanodendrites.

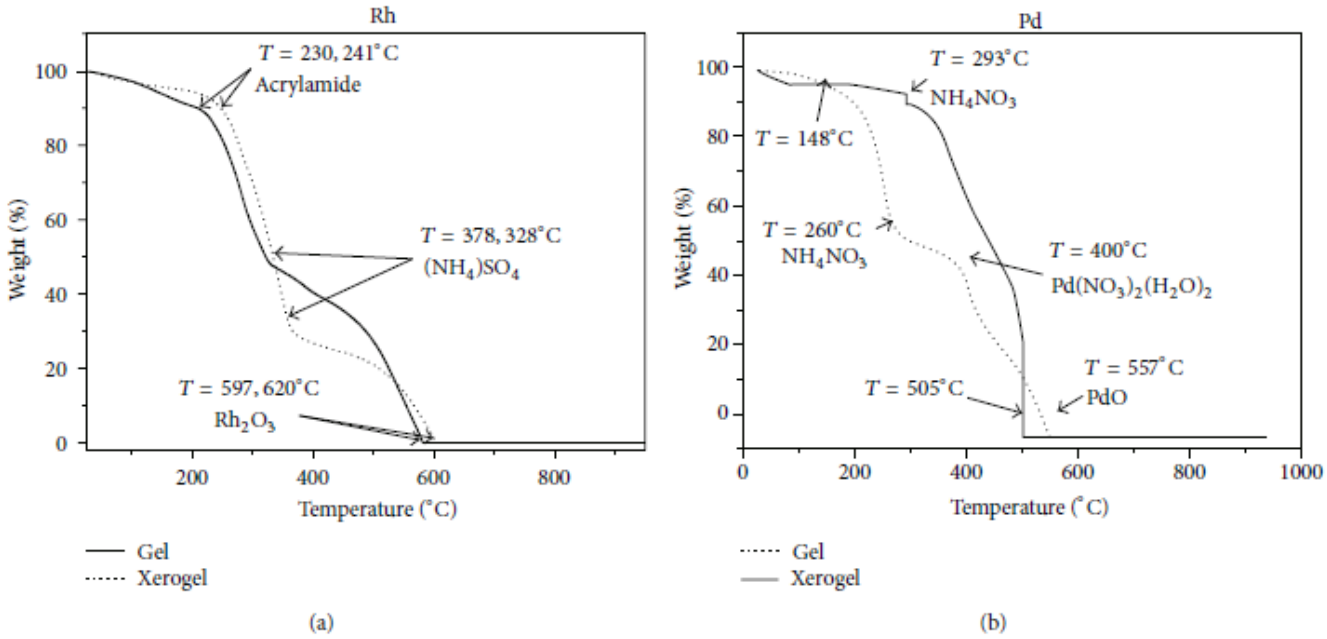

FIGURE 2: TGA curves from gel and xerogel for (a) rhodium and (b) palladium.

TABLE 1: Study of thermal transitions for the Rh and Pd gel and xerogel, respectively.

Rhodium thermal transition	Gel T (°C)	Xerogel T (°C)	Gel weight loss (%)	Xerogel weight loss (%)
Removal of the polymer (acrylamide)	241	230	13	9
Elimination of $(NH_4)_2SO_4$ compound	328	378	76	82
Rh_2O_3 formation	620	597	99	99
Palladium thermal transition	**Gel T (°C)**	**Xerogel T (°C)**	**Gel weight loss (%)**	**Xerogel weight loss (%)**
Removal of the polymer (acrylamide)	148	148	96	96
Elimination of $(NH_4)_2SO_4$ compound	273	300	56.2	92
Pd $(NO_3)_2(H_2O)_2$ formation	400	—	45	—
PdO decomposition	505	557	0.31	0.61

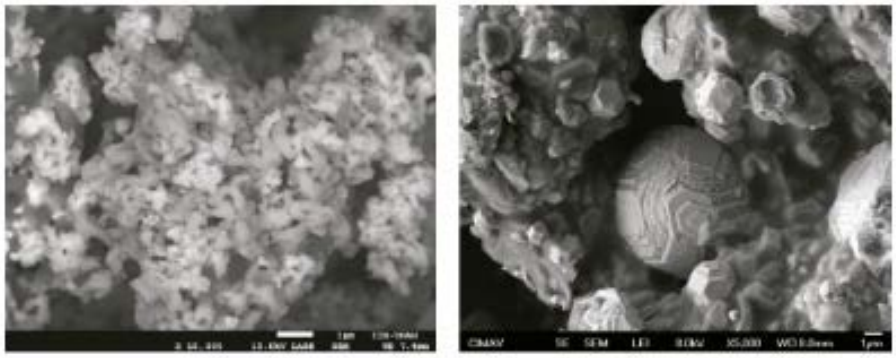

(a) (b)

FIGURE 3: SEM analysis for the (a) material before the heat treatment and (b) Rh-Pd alloy powders after applying the heat treatment at 1000°C for 2 h.

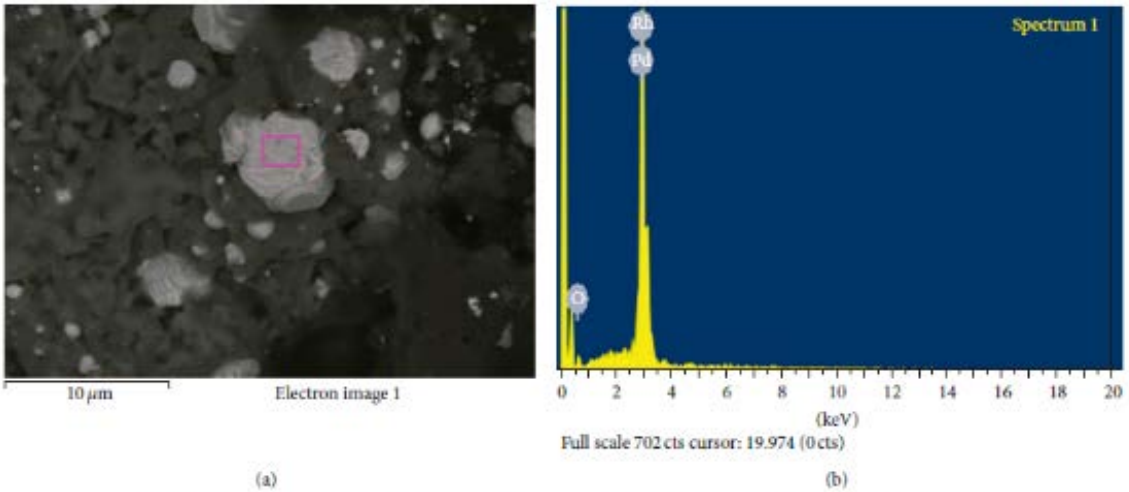

FIGURE 4: EDS analysis for the Rh-Pd alloy particles after applying the heat treatment at 1000°C for 2 h.

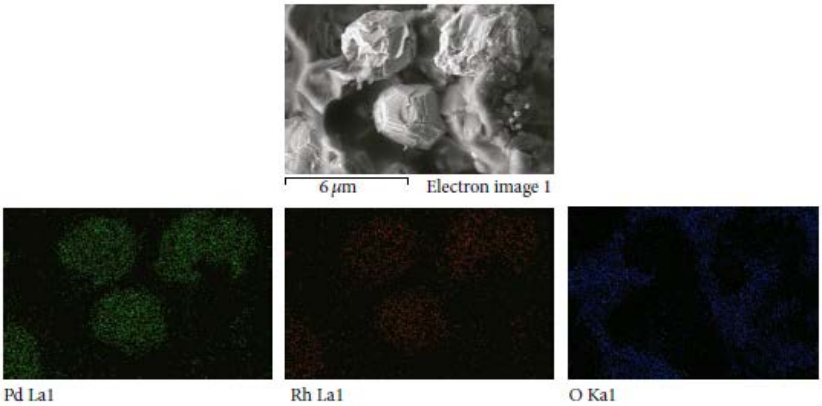

FIGURE 5: SEM elemental mapping for the bimetallic Rh-Pd.

These particles consisted of Rh branches anchored to a Pd nanocrystal core. The palladium nanocrystals synthesized by different methods exhibit distinct forms, that is, truncated octahedron, cube, and thin plate. According to Kobayashi, Pd has been successfully employed as seed to grow Rh branches. The bimetallic particles are around 20 nm. However, as mentioned above, the synthesized method used by Kobayashi is based on reducing Na_3RhCl_6 from Lascorbic acid in an aqueous solution. This method has several shortcomings; one of the most important is that varying the concentration of Na_3RhCl_6 during the synthesis could only control the degree of Rh branching. A high concentration of Rh in the solution causes that only part of Rh can be anchored around the Pd, and the excess of the produced nano-Rh, that fails to be anchored, is dispersed in the formed solution; that is, it fails to complete its reactions with Pd to form the bimetal. On the other hand, the varieties of morphologies, found by Kobayashi for Pd grains used as inoculants to grow the Rh branches, were comparable to those reported in this work for the synthesis of bimetallic Rh-Pd by the modified solgel technique. This could be attributed to the heat treatment applied, in which the sintering process of the bimetallic material begins, causing the grain growth, forming spherohexagonal shaped-like morphology particles. Besides, this method did help the formation of a bimetallic compound with a reasonably well homogeneous distribution, as it was clearly observed in the SEMmapping.

Conclusion

The reported microwave-assisted, sol-gel method was able to obtain nano-bimetallic Rh-Pd particles with an average size of 75 nm.Thermogravimetric analysis helped determine not only the decomposition temperatures but also the heat treatment

conditions needed to obtain nano-Rh-Pd-particles. After the heat treatment at 1000°C/2 h, the subproducts that were produced during the sol-gel reaction were removed. The synthesis of the nano-bimetallic Rh-Pd was confirmed by XRD and EDX.Th eHRTEM micrographs showed the formation of clusters with a polyhedron shape and distribution of the grains' size ranging from 50 to 200 nm. The clusters were successfully dispersed with an ultrasonic cleaner.The spherohexagonal shaped-like morphology particles reported in this work could be attributed to the heat treatment process. Finally, it is worth noting that our Rh-Pd particles are not restricted to a single application, as the resulting Rh-Pd nanoparticles were found to be free of impurities, since the stabilizer used (EDTA) was completely removed with the heat treatment.

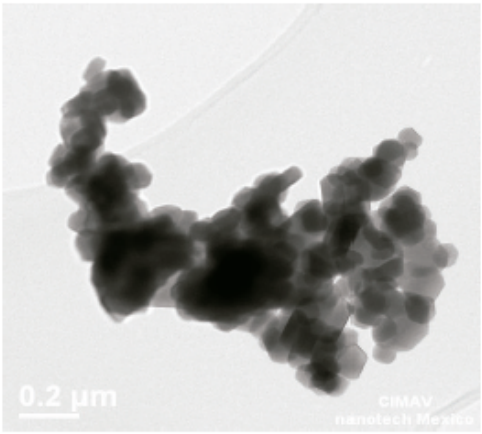

(a)

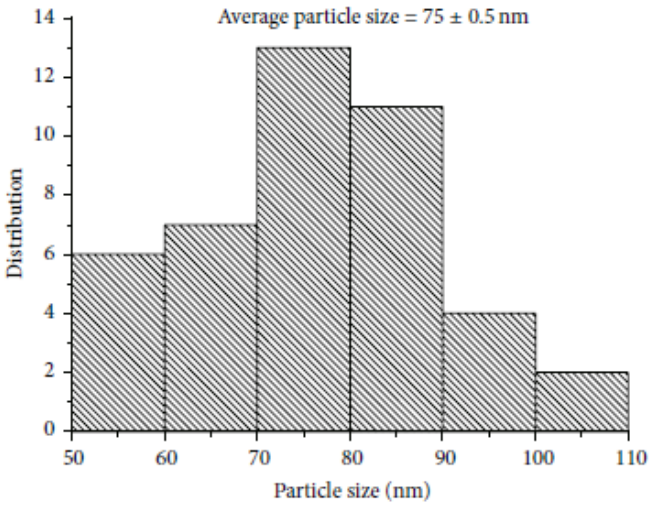

(b)

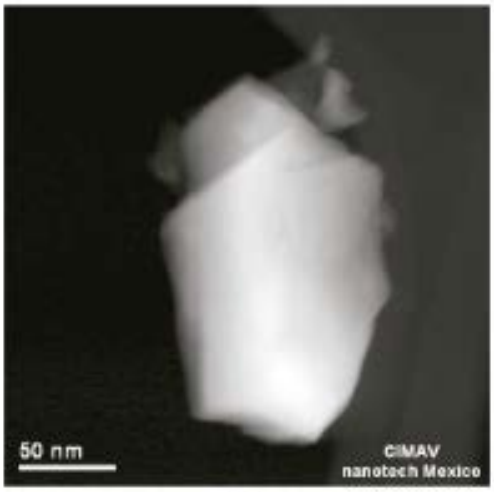

(c)

FIGURE 6: Micrographs of HRTEM of the nano-bimetallic Rh-Pd. (a) Sphero-hexagonal shapes, (b) average-size distribution of particles (~75 nm), and (c) grain of the bimetallic Rh-Pd of ~50 nm.

Acknowledgments:

M. Ugalde acknowledges the financial support from CONACyT through the scholarship 207277. I. A. Figueroa acknowledges the financial support from PAPIIT UNAM through project IB100712/RR180712. The authors also express their acknowledgment for the technical support of Laboratorio Nacional de Nanotecnología, Centro Nacional de Nanotecnología, and CIMAV and especially to Karla Campos Venegas, Carlos Ornelas, Omar Novelo, and Caín Gónzalez for their interesting useful discussions.

References:

[1] R. Ferrando, J. Jellinek, and R. L. Johnston, “Nanoalloys: from theory to applications of alloy clusters and nanoparticles,” Chemical Reviews, vol. 108, no. 3, pp. 845–910, 2008.

[2] T. Ragheb and L. A. Geddes, “Electrical properties of metallic electrodes,” Medical and Biological Engineering and Computing, vol. 28, no. 2, pp. 182–186, 1990.

[3] Q. Yuan and X. Wang, “Aqueous-based route toward noble metal nanocrystals: morphology-controlled synthesis and their applications,” Nanoscale, vol. 2, no. 11, pp. 2328–2335, 2010.

[4] H.-C. Kim, S.-M. Park, W. D. Hinsberg, and I. R. Division, “Block copolymer based nanostructures: materials, processes, and applications to electronics,” Chemical Reviews, vol. 110, no. 1, pp. 146–177, 2010.

[5] M.-C. Daniel and D. Astruc, “Gold nanoparticles: assembly, supramolecular chemistry, quantum-size-related properties, and applications toward biology, catalysis, and nanotechnology,” Chemical Reviews, vol. 104, no. 1, pp. 293–346, 2004.

[6] D. V. Talapin, J.-S. Lee, M. V. Kovalenko, and E.V. Shevchenko, “Prospects of colloidal nanocrystals for electronic and optoelectronic applications,” Chemical Reviews, vol. 110, no. 1, pp. 389– 458, 2010.

[7] N. F. Mott and H. Jones, Theory of the Properties of Metals and Alloys, Oxford University Press, London, UK, 1936.

[8] R. Coles, “Lattice spacings in Ni-Cu and Pd-Ag alloys,” Journal of the Institute of Metals, vol. 84, p. 346, 1956.

[9] A. Maeland and T. B. Flanagan, “Lattice spacings of goldpalladium alloys,” Canadian Journal of Physics, vol. 42, no. 11, pp. 2364–2366, 1964.

[10] T. B. Flanagan, B. Baranowski, and S. Majchrzak, “Remarkable interstitial hydrogen contents observed in rhodium-palladium alloys at high pressures,” Journal of Physical Chemistry, vol. 74, no. 24, pp. 4299–4300, 1970.

[11] B. Baranowski, S. Majchrzak, and T. B. Flanagari, “Diffusion of hydrogen in rhodium-palladiumalloys,” The Journal of Physical Chemistry, vol. 77, no. 23, pp. 2804–2807, 1973.

[12] B. Lim, Y. Xiong, Y. Xia et al., Journal ofMaterials Research, vol. 3, p. 1367, 1988, Angewandte Chemie International Edition, vol. 46, p.9279, 2007.

[13] B. Lim, M. Jiang, J. Tao, P. H. C. Camargo, Y. Zhu, and Y. Xia, “Shape-controlled synthesis of Pd nanocrystals in aqueous solutions,”Advanced Functional Materials, vol. 19,no. 2, pp. 189– 200, 2009.

[14] B. Lim, H. Kobayashi, P. H. C. Camargo, L. F. Allard, J. Liu, and Y. Xia, “New insights into the growth mechanism and surface structure of palladium nanocrystals,” Nano Research, vol. 3, no. 3, pp. 180–188, 2010.

[15] F.-R. Fan, D.-Y. Liu, Y.-F.Wu et al., “Epitaxial growth of heterogeneous metal nanocrystals: from gold nano-octahedra to palladium and silver nanocubes,” Journal of the American Chemical Society, vol. 130, no. 22, pp. 6949–6951, 2008.

[16] B. Lim, H. Kobayashi, P. H. C. Camargo, L. F. Allard, J. Liu, and Y. Xia, “New insights into the growth mechanism and surface structure of palladium nanocrystals,” Nano Research, vol. 3, no. 3, pp. 180–188, 2010.

[17] M. Rassoul, F. Gaillard, E. Garbowski, andM. Primet, “Synthesis and characterisation of bimetallic Pd-Rh/alumina combustion catalysts,” Journal of Catalysis, vol. 203, no. 1, pp. 232–241, 2001.

[18] K. Osseo-Asare and F. J. Arriagada, “Synthesis of nanosize particles in reverse microemulsions,” Ceramic Transactions, vol. 12, pp. 3–16, 1990.

[19] M. P. Pileni, “Reverse micelles as microreactors,” Journal of Physical Chemistry, vol. 97, no. 27, pp. 6961–6973, 1993.

[20] I. P. Beletskaya, A. N. Kashin, A. E. Litvinov, V. S. Tyurin, P. M. Valetsky, and G. Van Koten, “Palladium colloid stabilized by block copolymer micelles as an efficient catalyst for reactions of C-C and C-heteroatom bond formation,” Organometallics, vol. 25, no. 1, pp. 154–158, 2006.

[21] R.W. Siegel, S. Ramasamy,H.Hahn, Z. Li, T. Lu, and R. Gronsky, “Synthesis, characterization, and properties of nanophase TiO2,” Journal ofMaterials Research, vol. 3, no. 6, pp. 1367–1372, 1988.

[22] D.-H. Kim and J. Kim, “Synthesis of LiFePO4 nanoparticles in polyol medium and their electrochemical properties,” Electrochemical and Solid-State Letters, vol. 9, no. 9, pp. A439–A442, 2006.

[23] R. Uyeda, “The morphology of fine metal crystallites,” Journal of Crystal Growth, vol. 24-25, pp. 69–75, 1974.

[24] F. Robert, G. Oehme, I. Grassert, and D. Sinou, “Influence of amphiphile concentration on the enantioselectivity in the rhodium-catalyzed reduction of unsaturated substrates in water,” Journal ofMolecular Catalysis A, vol. 156, no. 1-2,pp. 127– 132, 2000.

[25] T.Mizuno, Y. Matsumura, T. Nakajima, and S. Mishima, “Effect of support on catalytic properties of Rh catalysts for steam reforming of 2-propanol,” International Journal of Hydrogen Energy, vol. 28, no. 12, pp. 1393–1399, 2003.

[26] A. Gniewek, A. M. Trzeciak, J. J. Zi´ołkowski, L. Ke¸pi´nski, J. Wrzyszcz, and W. Tylus, “Pd-PVP colloid as catalyst for Heck and carbonylation reactions: TEM and XPS studies,” Journal of Catalysis, vol. 229, no. 2, pp. 332–343, 2005.

[27] R. Narayanan and M. A. El-Sayed, “Effect of colloidal catalysis on the nanoparticle size distribution: dendrimer-Pd vs PVP-Pd nanoparticles catalyzing the Suzuki coupling reaction,” Journal of Physical Chemistry B, vol. 108, no. 25, pp. 8572–8580, 2004.

[28] V.V. Shumyantseva, S. Carrara, V. Bavastrelloet al., “Direct electron transfer between cytochrome P450scc and gold nanoparticles on screen-printed rhodium-graphite electrodes,” Biosensors and Bioelectronics, vol. 21, no. 1, pp. 217–222, 2005.

[29] I. Willner, R. Baron, and B. Willner, “Integrated nanoparticlebiomolecule systems for biosensing and bioelectronics,” Biosensors and Bioelectronics, vol. 22, no. 9-10, pp. 1841–1852, 2007.

[30] J. M. D. Zapiter, B. M. Tissue, and K. J. Brewer, “Ruthenium and rhodium complexes anchored to europium oxide nanoparticles,” Inorganic Chemistry Communications, vol. 11, no. 1, pp. 51–56, 2008.

[31] H. S. Nalwa, Handbook of Nanostructured Materials and Nanotechnology, vol. 1, Academic Press, San Diego, Calif, USA, 2000.

[32] M. Harada, D. Abe, and Y. Kimura, “Synthesis of colloidal dispersions of rhodium nanoparticles under high temperatures and high pressures,” Journal of Colloid and Interface Science, vol. 292, no. 1, pp. 113–121, 2005.

[33] J. Jimenez-Mier, G. Herrera, E. Chavira, L. Ba˜nos, J. Guzmán, and C. Flores, “Synthesis and structural characterization of YVO3 prepared by sol-gel

acrylamide polymerization and solid state reaction methods," Journal of Sol-Gel Science and Technology, vol. 46, no. 1, pp. 1–10, 2008.

[34] X.-D. Mu, J.-Q. Meng, Z.-C. Li, and Y. Kou, "Rhodium nanoparticles stabilized by ionic copolymers in ionic liquids: long lifetime nanocluster catalysts for benzene hydrogenation," Journal of the American Chemical Society, vol. 127, no. 27, pp. 9694–9695, 2005.

[35] T.Ashida, K.Miura, T.Nomoto et al., "Synthesis and characterization of Rh(PVP) nanoparticles studied by XPS andNEXAFS," Surface Science, vol. 601, no. 18, pp. 3898–3901, 2007.

[36] Y. Huang, J. Chen, H. Chen et al., "Enantioselective hydrogenation of ethyl pyruvate catalyzed by PVP-stabilized rhodium nanoclusters," Journal of Molecular Catalysis A, vol. 170, no. 1-2, pp. 143–146, 2001.

[37] J.-L. Pellegatta, C. Blandy, V. Colli`ere et al., "Catalytic investigation of rhodiumnanoparticles in hydrogenation of benzene and phenylacetylene," Journal of Molecular Catalysis A, vol. 178, no. 1-2, pp. 55–61, 2002.

[38] S. Morneta, S. Vasseura, F. Grassteb et al., "Magnetic nanoparticle design for medical applications," Progress in Solid State Chemistry, vol. 34, pp. 237–247, 2006.

[39] A. P. Alivisatos, "Semiconductor clusters, nanocrystals, and quantum dots," Science, vol. 271, no. 5251, pp. 933–937, 1996.

[40] U. Kreibig and M. Vollmer, Optical Properties of Small Metal Clusters, Springer, Berlin, Germany, 1995.

[41] B. Fegley Jr., P.White, and H. K. Bowen, “Processing and characterization of ZrO2 and Y-Doped ZrO2 powders,” American Ceramic Society Bulletin, vol. 64, no. 8, pp. 1115–1120, 1985.

[42] M. Ugalde, E. Chavira, M. T. Ochoa-Lara, and C. Quintanar, “New synthesis method to obtain Pd nano-crystals,” Journal of Nano Research, vol. 14, pp. 93–103, 2011.

[43] A. Sin and P. Odier, “Gelation by Acrylamide, a quasi-universal medium for the synthesis of fine oxide powders for electroceramic applications,” Advanced Materials, vol. 12, no. 9, pp. 649– 652, 2000.

[44] H.Wang, L. Gao, W. Li, andQ. Li, “Preparation of nanoscale α- Al2O3 powder by the polyacrylamide gel method,” Nanostructured Materials, vol. 11, no. 8, pp. 1263–1267, 1999.

[45] H.Kobayashi, B. Lim, J.Wang et al., “Seed-mediated synthesis of Pd-Rh bimetallic nanodendrites,” Chemical Physics Letters, vol. 494, no. 4–6, pp. 249–254, 2010.

[46] S.Kishore, J.A.Nelson, J.H. Adair, andP.C.Eklund, “Hydrogen storage in spherical and platelet palladium nanoparticles,” Journal of Alloys and Compounds, vol. 389, no. 1-2, pp. 234–242, 2005.